

Design, construction, and performance of a device for directional recrystallization of metallic alloys

J. M. Vallejos,^{1,2} M. E. Leonard,^{1,3} C. E. Sobrero,^{1,3} P. M. La Roca,¹ A. V. Druker,^{1,3} and J. A. Malarria^{1,3}

¹Instituto de Física Rosario (CONICET-UNR), 27 de Febrero 210 bis, 2000 Rosario, Argentina

²Facultad de Ingeniería, Universidad Nacional del Nordeste, Las Heras 727, 3500 Resistencia, Argentina

³Facultad de Ciencias Exactas, Ingeniería y Agrimensura, Universidad Nacional de Rosario, Ave. Pellegrini 250, 2000 Rosario, Argentina

(Received 23 September 2016; accepted 17 January 2017; published online 8 February 2017)

A device was designed to apply the directional recrystallization method to Fe-based alloys in order to obtain bamboo-like microstructures. This microstructure is suitable for improving creep properties and resistance to fatigue in some alloys and for enhancing pseudoelastic properties in shape memory alloys. The design and construction of a flat coil are described in detail. In addition, we developed an electromechanical system to control the movement of a wire within the flat coil. The construction details and system performance are presented. Furthermore, metallographic studies taken from the directionally recrystallized low-carbon steel samples are shown. Nearly monocrystalline and bamboo-like microstructures were achieved in the steel wires. *Published by AIP Publishing.* [<http://dx.doi.org/10.1063/1.4975179>]

I. INTRODUCTION

With elongated grains parallel to the tensile direction, columnar-grained microstructures can improve creep properties, fatigue resistance, and impart crack-stopping behavior in metallic alloys.^{1–3} These kinds of microstructures can be obtained by either of the two methods: directional solidification or directional recrystallization. The first process consists of melting a small region of wire and moving it towards a chill zone, in order to develop the directional solidification. For the second method, the hot-zone temperature is not enough to melt the material, and the strong thermal gradient, which moves across the sample, promotes preferential grain growth, achieving directional grain recrystallization. The second method processes the material in the solid state without the need of melting parts of the alloy. This provides an advantage over directional solidification techniques.

The floating-zone technique, developed by Theuerer in 1962,⁵ was first used to produce silicon single crystals.⁴ Keck and Müller applied high frequency induction heating⁶ to the process and Buehler developed an automatic floating-zone gas-refining apparatus for processing silicon. He managed to grow 13 mm long crystals.⁷ Based on Buehler's system, Wernick *et al.* applied this technique to the refinement of Ni, Ti, and V.⁸ During the last few decades, several improvements to the original system have been made, in order to reduce dislocation densities and increase the crystal size.⁴

Material parameters such as grain size, texture, and impurity content strongly affect the directional recrystallization (DR)^{9–12} of grains. Some of the first applications of the DR technique were intended to improve the mechanical properties of iron-base superalloys.^{11,13,14} To achieve a columnar-grain microstructure in these alloys, an initial matrix of small equiaxed grains is necessary.^{13,15} Some process parameters, such as drawing velocity, thermal

gradient, and hot-zone width, also have a significant influence on the columnar grain growth.^{12,16–19} For a columnar-grained microstructure to form and propagate, the hot zone must move at a slower speed than that corresponding to the grain-boundary migration.¹⁷ Using this technique, Zhang *et al.* grew elongated-grain microstructures 23 mm long with an aspect ratio (relationship between the length and width of a grain) of 60 in commercially purity iron that did not have deformation energy accumulated in the matrix or a previous texture.¹⁶

A bamboo-like microstructure, which consists of a few coarse grains, larger than the specimen width, is another result of the abnormal grain growth. This microstructure, as well as columnar-type grains, can increase fatigue resistance in some alloys.^{20,21} In addition, magnetic and electrical properties are improved by this morphology in materials as Cu or Ni–Mn–Ga microwires.^{22,23} Also bamboo-like microstructures enhance pseudoelastic properties in a wide range of shape memory alloys due to anisotropic transformation strain behavior and incompatibility between neighboring grains.^{24–26}

Some complex methods have been applied to produce bamboo-like microstructures.^{22,27} In spite of its simplicity, DR has not been used to generate this microstructure in alloys whose functional, pseudoelastic, or mechanical properties are improved by achieving such a morphology. There are two important parameters in the process that strongly affect the width of the columnar-grained microstructure: the drawing velocity and the width of the hot-zone.¹⁷ A wider hot zone promotes the formation of a growth front and due to this, both the width and length of the columnar grains increase with increasing hot-zone width. By decreasing the hot-zone velocity, a similar effect is produced in the microstructure. Thereby, it is possible to set these two parameters for the material to have enough time of residence in the hot zone to obtain grain widths larger than the sample width. In this way, a

bamboo-like microstructure of elongated grains is achieved by the DR process.

The aim of this work was to develop a simple device that allows us to directionally grow grains into a bamboo-like microstructure in Fe-based alloys. A simple design was sought so that the method can be reproduced on an industrial scale. The design and construction of a flat coil, specifically intended to work in conjunction with induction heating, are described in detail. In addition, we developed and present here an electromechanical system to control the movement of a wire within the flat coil. Finally, in Section III, preliminary results demonstrating the device's performance are given.

II. DESIGN

The system's characteristics and performance follow:

- (1) Construction using readily available materials.
- (2) A drawing velocity ranging between 5 and 80 $\mu\text{m/s}$ (in which the growth of columnar grains for commercial pure iron is achieved¹⁶).
- (3) Heat treatment of wires up to 5 mm in diameter.

The induction heater has a high frequency current source that combines vacuum valves and solid state frequency converters. A summary of the equipment characteristics is given below.

- Power: 3 kW
- Heating frequency: 300 kHz
- AC line frequency: 50 Hz
- Anode voltage: 3.5 kV
- Supply voltage: 380 V

A. Flat coil

A flat coil was designed to generate a localized heating zone within the test material. To obtain the highest performance from induction heating it is necessary that the impedance of the coil be equal to the impedance of the oscillating internal circuit.²⁸ Therefore the flat coil was designed in order that its inductance was approximately equal to the inductance of the system's original coil (0.185 μH).

To obtain local heating, the coil was arranged as a flat spiral or "pancake," where several turns are wound in the same plane. The coil was fabricated from commercial copper tubing 7.938 mm in diameter. The inner diameter of the flat coil was wound to 8 mm, to provide the necessary space for the motion of a 5 mm diameter wire and to have a separation of 1 mm between adjacent turns (corresponding to the thickness of the insulation). The inductance L and the auxiliary parameter A necessary to determine its value were calculated for different numbers of turns using Equations (1) and (2),²⁹ where N is the number of turns, and d , s , D , and w are the dimensions shown in Fig. 1(a). The inductance values obtained from these calculations are summarized in Table I,

$$L = \frac{N^2 \times A^2}{30A - 11d}, \quad (1)$$

$$A = \frac{d + N \times (w + s)}{2}. \quad (2)$$

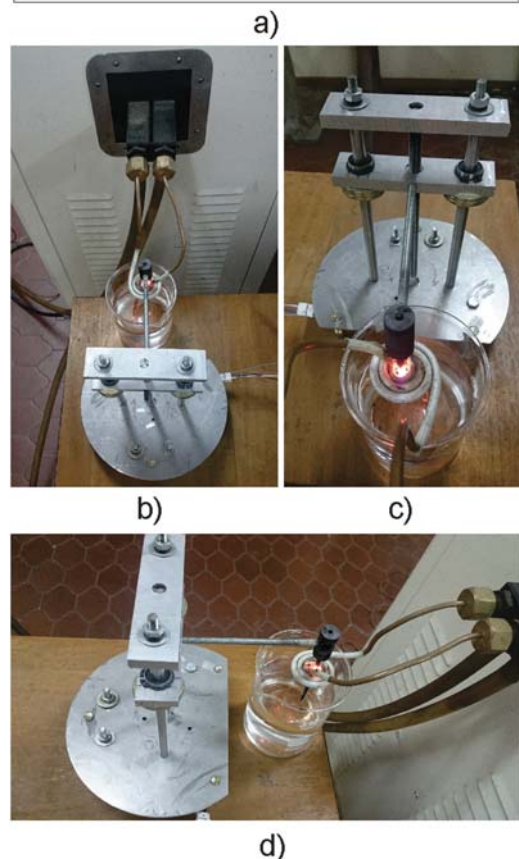
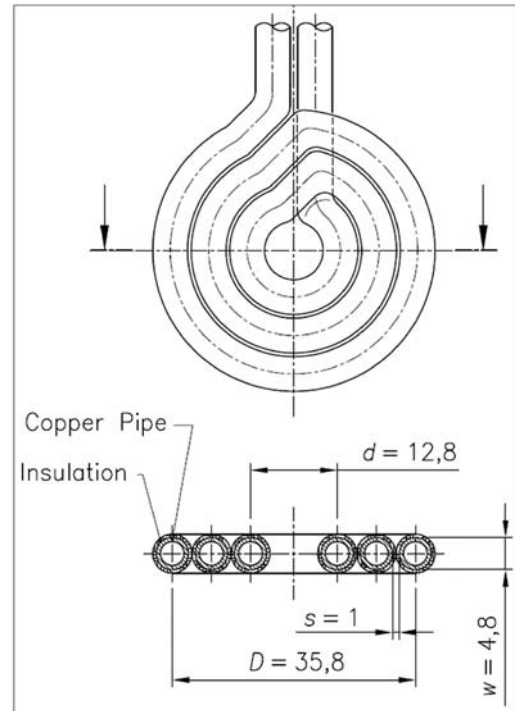


FIG. 1. (a) Schematic drawing of the flat coil. (b) Top view of the system. (c) Front view of the system. (d) Side view of the system. All dimensions are in millimeters.

Although the inductance value closest to the original (0, 185 μH) is obtained with two turns, a three-turn configuration was used to reduce the current and avoid overheating problems in the inductor. Drawings of the coil and images of the wire

TABLE I. Inductance values of the spiral coil for different numbers of turns (μH).

Number of turns	Inductance value (H)
1	0.103
2	0.257
3	0.508

pulling device coupled to the induction system are shown in Figure 1.

B. Electromechanical device to control the motion of a wire moving through the flat coil

In order to control the linear motion of a wire passing through the flat coil, an electromechanical system was developed. The parts constituting this system will work with samples of different materials and geometries. For the present work, the device was developed to operate within the velocity range producing columnar grain growth for pure iron.¹⁶ The motion is provided by a unipolar stepping motor operating at 48 steps per revolution. This motor operates between 35 and 650 rpm and is controlled by an Arduino UNO board and an array of Darlington transistors. A gear train with three linked reduction stages (5:1, 5:1, and 8.33:1) was coupled to the stepping motor. Thus, a total reduction of approximately 208:1 is obtained. A 9.525 mm threaded rod was coupled to the output axis of the reduction train. The linear movement is accomplished by a crosshead with a nut fixed in the middle, which is moved through rotation of the threaded rod. Two linear bearings were mounted on the extremes of the crosshead. These bearings slide on the supporting frame's vertical honed rods. The maximum and minimum drawing velocities V can be calculated with Equation (3). This formula can also be used to calculate the total velocity reduction needed for the application of DR in different materials. The drawings of the mechanism are shown in Figure 2. In order to get columnar grains or bamboo-like structures for different alloys, a small variation to the gear train should be performed, taking into account the velocity of grain growth for each material,

$$V \left[\frac{\text{mm}}{\text{min}} \right] = n \left[\frac{\text{rev}}{\text{min}} \right] \times \text{Gear Reduction} \times \text{Lead} \left[\frac{\text{mm}}{\text{rev}} \right], \quad (3)$$

$$V_{\min} = 35 \left[\frac{\text{rev}}{\text{min}} \right] \times \frac{1}{208.33} \times \frac{25.4}{16} \left[\frac{\text{mm}}{\text{rev}} \right] \\ \times \frac{1000}{1} \left[\frac{\mu\text{m}}{\text{mm}} \right] \times \frac{1}{60} \left[\frac{\text{min}}{\text{seg}} \right],$$

$$V_{\min} = 4.45 \left[\frac{\mu\text{m}}{\text{seg}} \right],$$

$$V_{\max} = 650 \left[\frac{\text{rev}}{\text{min}} \right] \times \frac{1}{208.33} \times \frac{25.4}{16} \left[\frac{\text{mm}}{\text{rev}} \right] \\ \times \frac{1000}{1} \left[\frac{\mu\text{m}}{\text{mm}} \right] \times \frac{1}{60} \left[\frac{\text{min}}{\text{seg}} \right],$$

$$V_{\max} = 82.55 \left[\frac{\mu\text{m}}{\text{seg}} \right].$$

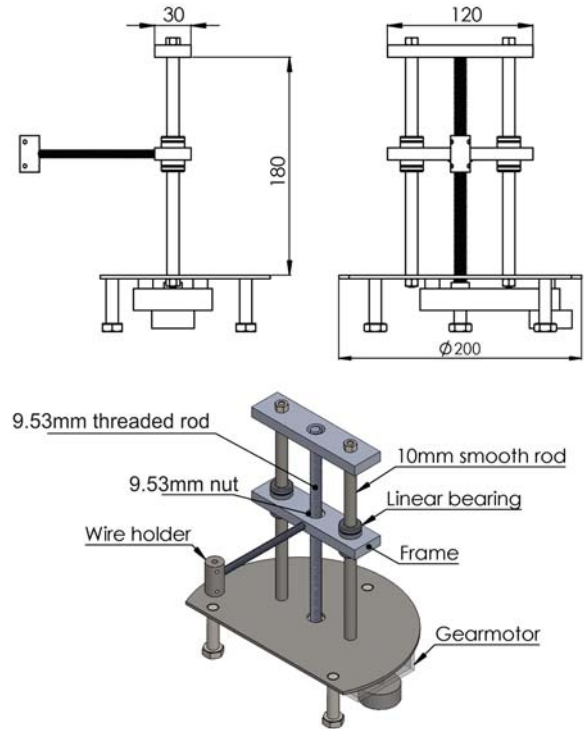


FIG. 2. Drawings of the electromechanical system to control the motion of a wire passing through the flat coil. All dimensions are in millimeters.

C. Materials and methods of testing

The DR method was applied to low-carbon steel wires 1.4 mm in diameter, with drawing velocities of 10, 15, and 20 $\mu\text{m/s}$. The Hot Zone Temperature (HZT), the temperature of the material inside the coil, was set at 750 °C. A cube with room temperature water, chill block, was used to create a controlled temperature gradient within the wire. This cooling system is simpler than the recirculating Ga–In liquid system used by Zhang *et al.*¹² Due to the small sample sizes, no temperature variation in the chill block water was observed during tests lasting longer than 2 h. To treat bigger specimens, a cooling system can be added to the chill block or, in case that a different temperature gradient is needed, commercial quenching oil can be used. The distance between the cooling water and the flat coil was adjusted to have a gradient of approximately 20 °C/mm for all samples. The wire's temperature was measured with a welded thermocouple.

The microstructures generated in these directional heating experiments were studied with optical metallography. All the processed samples were mechanically polished and etched with 7% nitric acid and 93% ethylic alcohol. The metallographic images were obtained with an Olympus PME3 optical microscope.

III. PERFORMANCE

The magnetic energy losses due to flux dispersion between the coil and the specimen reduce the final temperature that can be achieved in the sample. Figure 3 shows the HZT of low-carbon steel wires as a function of the wire diameter. It

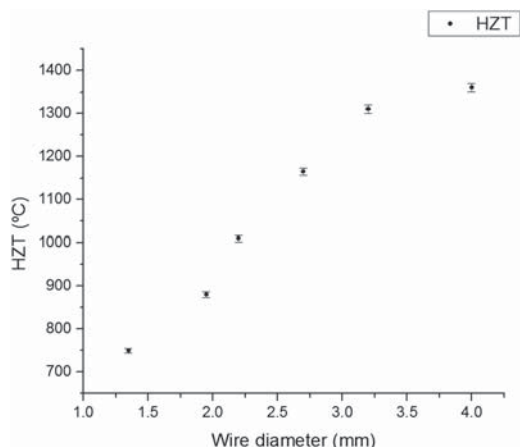


FIG. 3. HZT as a function of the low-carbon steel wire diameter, at full power.

can be seen that the reduction of the sample size produces an abrupt decrease of the HZT for wires less than 3 mm in diameter.

A strong temperature gradient in the material is essential to produce columnar-grained structures by the DR process. If it is achieved, the recrystallization and movement of grain boundaries occur only in grains near the coil. The measured temperature gradient in a 1.4 mm diameter wire, with a distance of 50 mm between the centre of the coil and the chill block, is shown in Figure 4. There is a primary zone (Zone I in Figure 4) near the coil approximately 10 mm in long where the temperature remains almost constant, decreasing only 2.2 °C/mm. This wide hot zone promotes the columnar grain growth, both in width and in length.¹⁷ Below Zone I, the temperature gradient remains almost constant in the parts of the sample that are farther away from the coil, with an average value of 16.4 °C/mm (Zone II in Figure 4). This gradient can be considered constant even though the chill block cooling water is not circulated. This is because the volume of water in the chill block is much larger than the hot material portion of the wire. The water temperature only varied 1 °C during 2 h of testing.

The original microstructure of the wire is shown in Figure 5. The wire had an average grain size of about 10 μm, as determined by the linear intercept method. Figure 6 shows the microstructures of the specimens directionally annealed

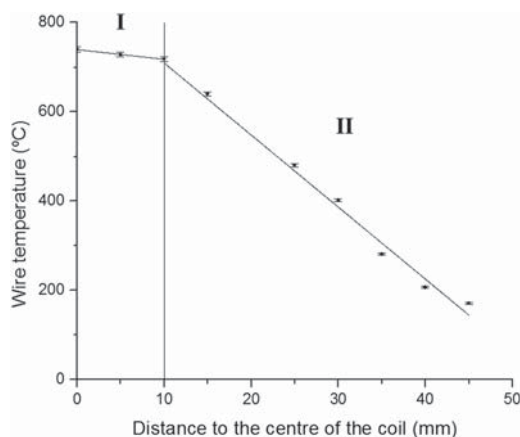


FIG. 4. Temperature gradient in a 1.4 mm diameter wire.

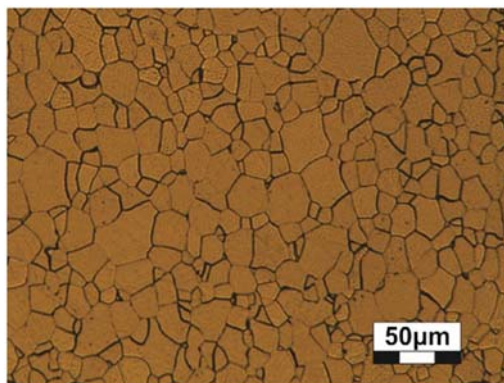


FIG. 5. Microstructure of the starting material.

at 750 °C with drawing velocities of 20, 15, and 10 μm/s. Abnormally shaped grains, elongated in the direction of the wire’s movement, were found in all samples. In specimens annealed at a pull rate of 20 μm/s, an abnormal growth of some grains was observed over wide regions of the wires. However, the propagation of the columnar structure along the entire sample was not achieved under this condition. The largest crystals were surrounded by small grains of a similar size to the original microstructure. The maximum grain length observed was 3 mm, and the average aspect ratio of the abnormally grown grains was 5. Bamboo-like structures were produced in wires annealed at a drawing velocity of 15 μm/s, as shown in Figure 6(b). In this case, the abnormal grain growth was sustained over the entire length of the treated specimen. Furthermore, almost monocrystalline microstructures were achieved in samples annealed at a velocity of 10 μm/s. The maximum length of the grains observed was 7 mm. It should be mentioned that all directionally annealed samples contain some isolated grains inside of the abnormally grown crystals. These small grains remain pinned maybe due to a

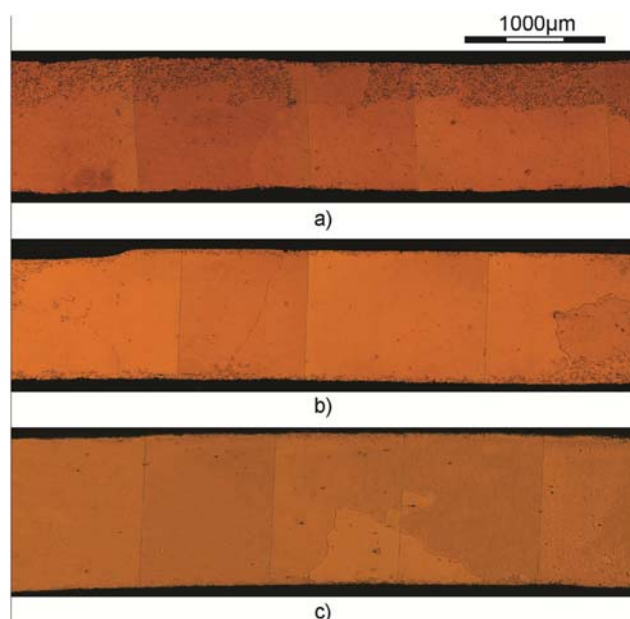


FIG. 6. Microstructure of the low-carbon steel wire directionally annealed at velocities of: (a) 20 μm/s; (b) 15 μm/s; (c) 10 μm/s.

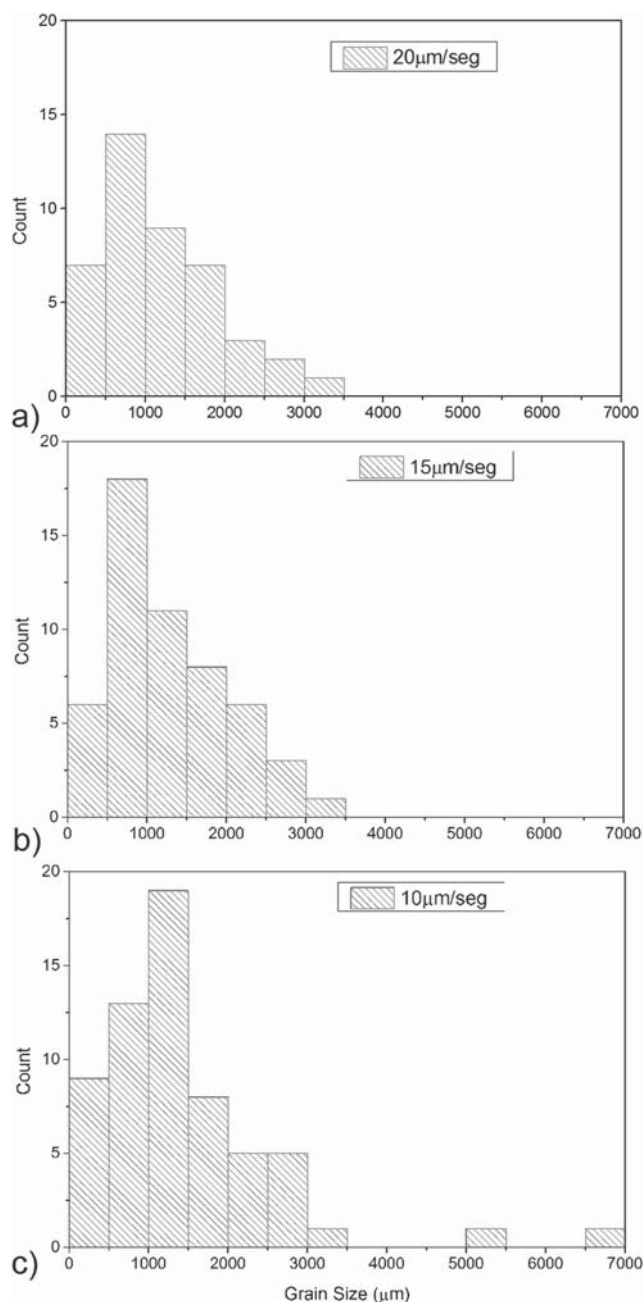


FIG. 7. Grain size distribution of the low-carbon steel wire directionally annealed at velocities of (a) 20 $\mu\text{m/s}$; (b) 15 $\mu\text{m/s}$; (c) 10 $\mu\text{m/s}$.

low migration velocity for low angle grain and twin boundaries.^{12,16,18} The grain size distributions of the specimens directionally annealed at 750 °C with drawing velocities of 20, 15, and 10 $\mu\text{m/s}$ are shown in Figure 7, in the form of histograms. The samples directionally annealed at velocities of 20 and 15 $\mu\text{m/s}$ have a similar grain-size distribution with a majority of grains between 500 and 1000 μm long. Samples annealed at a velocity of 10 $\mu\text{m/s}$ have longer grains, the majority between 1000 and 1500 μm , although grains 5200 and 6500 μm long were observed. It should be noted that the longest grain obtained in the present work, 7 mm, is larger than the one grown by Zhang *et al.*¹⁶ at the same HZT and drawing velocity. This is due to the wider hot-zone width of our apparatus.

IV. CONCLUSIONS

In this paper, a system to apply the floating zone and directional recrystallization processes to metal alloys is presented. This system can be used to process wires up to 5 mm in diameter over a range of drawing velocities between 5 and 80 $\mu\text{m/s}$. Directional recrystallization experiments were carried out on low-carbon steels under different conditions. Semi-columnar grain microstructures were realized in specimens 1.4 mm in diameter moving through the induction coil at 20 $\mu\text{m/s}$. The largest grains had a length of 1.5 mm and an aspect ratio of 5. In other experiments, bamboo-like structures developed in low-carbon steel samples drawn at 10 and 15 $\mu\text{m/s}$. In these experiments, the largest crystals reached a length of approximately 7 mm.

The understanding of the processing parameters for growing large crystals in metals and the mechanisms of abnormal grain growth are broad fields of research receiving a great deal of interest. The system presented in this paper illustrates a low-cost technique that can be used to obtain the abnormal grain growth through steep temperature gradients in metal alloys.

ACKNOWLEDGMENTS

This work was supported by the CONICET (Argentina) through grants PDTs 251 and PIP 0488. The authors wish to thank Dr. M. Stout for proofreading this manuscript. We are also grateful to H. Rindizbacher and D. Castellani for technical assistance.

- ¹R. L. Cairns, L. R. Curwick, and J. S. Benjamin, *Metall. Mater. Trans. A* **6**, 179 (1975).
- ²A. W. Godfrey and J. W. Martin, *Mater. Sci. Eng.: A* **222**, 91 (1997).
- ³A. Tekin, M. Mujahid, J. W. Martin, S. W. K. Shaw, G. M. McColvin, and L. C. Elliott, in *Superalloys*, edited by S. D. Antolovich (TMS, Warrendale, 1992), p. 457.
- ⁴A. Mühlbauer, in *Modelling for Material Processing: Proceedings of the 4th International Scientific Colloquium, Riga, Latvia, 8–9 June 2006*, edited by A. Jakovics (University of Latvia, Riga, 2006), pp. 13–20.
- ⁵H. C. Theuerer, U.S. patent 3,060,123 (23 October 1962).
- ⁶P. H. Keck, W. van Horn, and J. Soled, *Rev. Sci. Instrum.* **25**, 331 (1954).
- ⁷E. Buehler, *Rev. Sci. Instrum.* **28**, 453 (1957).
- ⁸J. H. Wernick, D. Dorsi, and J. J. Byrnes, *J. Electromech. Soc.* **106**, 245 (1959).
- ⁹I. Baker and J. Li, *Acta Mater.* **50**, 805 (2002).
- ¹⁰J. Li and I. Baker, *Mater. Sci. Eng.: A* **392**, 8 (2005).
- ¹¹T. S. Chou and H. K. D. H. Badheshia, *Mater. Sci. Eng.: A* **189**, 229 (1994).
- ¹²Z. W. Zhang, G. Chen, and G. L. Chen, *Mater. Sci. Eng.: A* **422**, 241 (2006).
- ¹³J. M. Marsh and J. W. Martin, *Mater. Sci. Technol.* **7**, 183 (1991).
- ¹⁴T. Tsuyimoto, T. Matsui, T. Suzuki, Y. Tomota, K. Shibue, and K. Furuyma, *Intermetallics* **9**, 97 (2001).
- ¹⁵A. O. Humphreys, S. W. K. Shaw, and J. W. Martin, *Mater. Charact.* **34**, 9 (1995).
- ¹⁶Z. W. Zhang, G. Chen, and G. L. Chen, *Acta Mater.* **55**, 5988 (2007).
- ¹⁷A. Y. Badmos, H. J. Frost, and I. Baker, *Acta Mater.* **50**, 3347 (2002).
- ¹⁸Z. W. Zhang, G. Chen, and G. L. Chen, *Mater. Sci. Eng.: A* **435-436**, 573 (2006).
- ¹⁹Z. W. Zhang, G. Chen, and G. L. Chen, *Mater. Sci. Eng.: A* **434**, 58 (2006).
- ²⁰H. Margolin, Y. Mahajan, and Y. Saleh, *Scr. Metall.* **10**, 1115–1118 (1976).
- ²¹S. M. Ueland and C. A. Schuh, *Acta Mater.* **60**, 282–292 (2012).

- ²²P. Zheng, N. J. Kucza, C. L. Patrick, P. Müllner, and D. C. Dunand, *J. Alloys Compd.* **624**, 226–233 (2015).
- ²³V. Carreaux, S. Maitrejean, M. Verdier, Y. Bréchet, A. Roule, A. Toffoli, V. Delaye, and G. Passemard, *Microelectron. Eng.* **84**, 2723–2728 (2007).
- ²⁴C. E. Sobrero, P. La Roca, A. Roatta, R. E. Bolmaro, and J. Malarría, *Mater. Sci. Eng.: A* **536**, 207–215 (2012).
- ²⁵T. Omori, M. Okano, and R. Kainuma, *APL Mater.* **1**, 032103 (2013).
- ²⁶M. Vollmer, P. Krooß, M. J. Kriegel, V. Klemm, C. Somsen, H. Özcan, I. Karaman, A. Weidner, D. Rafaj, H. Biermann, and T. Niendorf, *Scr. Mater.* **114**, 156 (2016).
- ²⁷P. Zheng, N. J. Kucza, Z. Wang, P. Müllner, and D. C. Dunand, *Acta Mater.* **86**, 95–101 (2015).
- ²⁸P. A. Hassell and N. V. Ross, *ASM Handbook Volume 4: Heat Treating of Steel* (ASM International, Youngstown, 2011), p. 164.
- ²⁹H. A. Wheeler, *Proc. Inst. Radio Eng.* **16**, 1398 (1928).